NANO LETTERS
Cite This: Nano Lett. 2019, 19, 7464−7469
Letter
pubs.acs.org/NanoLett

Light Polarization-Controlled Conversion of Ultrafast Coherent−Incoherent Exciton Dynamics in Few-Layer ReS_2

Sangwan Sim,[†,▽] Doeon Lee,[‡,▽] Jekwan Lee,[§] Hyemin Bae,[○] Minji Noh,[§] Soonyoung Cha,[∥] Moon-Ho Jo,[∥,⊥] Kyusang Lee,[‡,#] and Hyunyong Choi*[,§]

[†]Division of Electrical Engineering, Hanyang University, Ansan 15588, Korea
[‡]Department of Electrical and Computer Engineering, University of Virginia, Charlottesville, Virginia 22903, United States
[§]Department of Physics and Astronomy, Seoul National University, Seoul 08826, Korea
[∥]Center for Artificial Low Dimensional Electronic Systems, Institute for Basic Science (IBS), Pohang 3767, Korea
[⊥]Department of Materials Science and Engineering, Pohang University of Science and Technology (POSTECH), Pohang 37673, Korea
[#]Departments of Materials Science and Engineering, University of Virginia, Charlottesville, Virginia 22903, United States
[○]School of Electrical and Electronic Engineering, Yonsei University, Seoul 03722, Korea

Supporting Information

ABSTRACT: Coherent light−matter interaction can transiently modulate the quantum states of matter under nonresonant laser excitation. This phenomenon, called the optical Stark effect, is one of the promising candidates for realizing ultrafast optical switches. However, the ultrafast modulations induced by the coherent light−matter interactions usually involve unwanted incoherent responses, significantly reducing the overall operation speed. Here, by using ultrafast pump−probe spectroscopy, we suppress the incoherent response and modulate the coherent-to-incoherent ratio in the two-dimensional semiconductor ReS_2. We selectively convert the coherent and incoherent responses of an anisotropic exciton state by solely using photon polarizations, improving the control ratio by 3 orders of magnitude. The efficient modulation was enabled by transient superpositions of differential spectra from two nondegenerate exciton states due to the light polarization dependencies. This work provides a valuable contribution toward realizing ideal ultrafast optical switches.

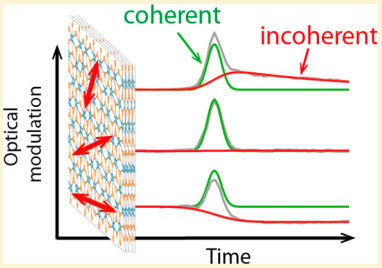

KEYWORDS: *Ultrafast exciton dynamics, coherent light−matter interaction, two-dimensional transition metal dichalcogenides, rhenium disulfide*

The optical stark effect (OSE) describes modulations of quantum energy states via coherent light−matter interactions.[1−4] Upon nonresonant laser excitation, a photon-dressed state is created, which repulsively interacts with a quantum state of matter, resulting in transient changes in the energy level (left panel in Figure 1a). This interaction accompanies a shift in absorption resonance of the state (Figure 1b), leading to transient changes in the fundamental optical properties, such as transmittance and reflectance. Because the OSE originates from the coherence between light and matter, optical modulation directly follows the temporal envelope of the incident short laser pulse, enabling ultrafast modulation on femtosecond time scales as illustrated by the green line in Figure 1c. Therefore, the OSE has been considered as a promising strategy for realizing femtosecond optical switches and has therefore been intensively studied in various condensed matter systems, such as III−V semiconducting quantum wells,[4−7] low-dimensional semiconductors,[8−14] and perovskite materials.[15]

However, there is a critical difficulty impeding the implementation of ideal OSE devices. Because the Stark shift is proportional to light intensity,[1] it generally requires a fairly strong laser pulse to induce an observable OSE. Thus, although photon energies of laser pulses are usually lower than bandgaps of materials, significant amounts of carriers are generated by two-photon absorption, resulting in extremely slow incoherent dynamics lasting for a long duration even after the laser pulse has passed the material (red line in Figure 1c). Such phenomena have been observed in most of the OSE materials studied so far,[5,6,8,9,15,16] significantly inhibiting the modulation speed. Therefore, if the incoherent component can be suppressed or controlled, this may provide an important contribution to realizing ideal ultrafast OSE devices.

Rhenium disulfide (ReS_2) is a member of the layered two-dimensional transition metal dichalcogenide (2D TMD) family.[17−26] This material exhibits strongly anisotropic excitons due to its low in-plane-symmetry crystal lattice. Recently, we found that the anisotropic excitons in few-layer ReS_2 exhibit strong coherent light−matter interactions including OSE and

Received: August 2, 2019
Published: August 26, 2019

DOI: 10.1021/acs.nanolett.9b03173
Nano Lett. 2019, 19, 7464−7469

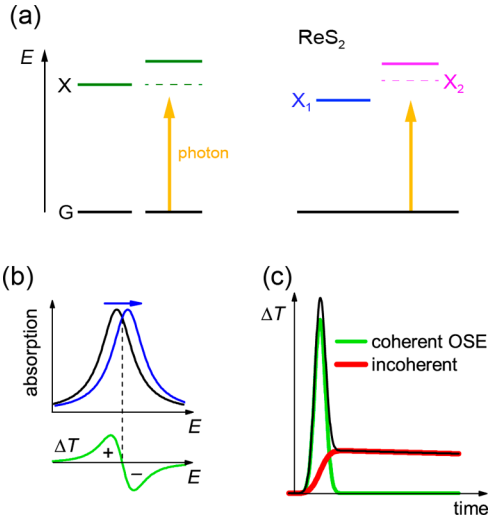

Figure 1. Coherent and incoherent light−matter interactions. (a) Left: description of the OSE in a two-level system. Black and green lines represent energy levels of the ground (G) and excited (X) states, respectively. The nonresonant optical excitation (yellow arrow) induces a shift in the excited state via the coherent light−matter interaction. Right: OSE of anisotropic excitons (X_1 and X_2) in ReS_2. We suppress the incoherent response occurring after the optical Stark shift in X_2 by using photon polarization. This method is based on the spectral superposition of resonance broadening of these two excitons with different polarization dependencies (see main text). (b) The black and blue lines represent the unperturbed and Stark-shifted absorption spectra, respectively. The green line shows a corresponding DT profile. (c) The DT dynamics typically observed in OSE experiments (black line). These dynamics usually include both the ultrafast OSE (green line) and relatively slow incoherent response (red line).

quantum beats.[8,27] In particular, manipulations of those coherent phenomena were possible by utilizing unique features of ReS_2 in that its anisotropic excitons are energetically nondegenerate but have completely different optical selection rules. However, similar to most of the other OSE materials, the slow incoherent response following the OSE has also remained an unresolved issue in ReS_2.[8]

Here, we present an ultrafast pump−probe spectroscopy experiment on selective conversion between the coherent OSE and the incoherent response in a few-layer ReS_2. By using only laser polarizations, we almost completely suppress and control the incoherent response to maximize the coherent-to-incoherent ratio for the second lowest anisotropic exciton state (right panel in Figure 1a). This modulation is based on the interplay of two exciton states with different light-polarization dependencies. This study provides a new way for selective control of two optical responses with completely different time scales.

The ultrafast pump−probe spectroscopy utilized in this experiment is based on a 250 kHz Ti:sapphire regenerative amplifier system centered at 800 nm with output pulses of a 50 fs time duration that are split into two branches. The first branch is used as a pump, which is bandpass filtered at 810 nm to excite only the lowest exciton state at 1.532 eV. The pump fluence is fixed at 115 $\mu J\ cm^{-2}$. The second branch is focused into a sapphire disk to generate a white-light probe beam. The probe beam transmits the sample and passes through a monochromator, then reaches a photodiode that measures the differential transmission (DT). DT is defined by $\Delta T/T$, where T is the probe intensity without the pump and ΔT is its change due to the pump excitation. DT traces are recorded as a function of the time delay Δt between the pump and probe. All of the optical measurements were performed at 78 K.

Six to seven layers of ReS_2 flake on a sapphire substrate were prepared by the mechanical exfoliation method (Figure 2a).

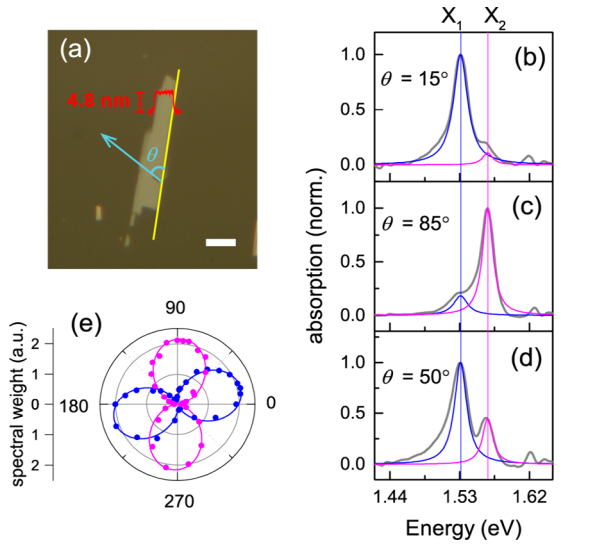

Figure 2. Steady-state optical characterization. (a) Optical image of ReS_2 sample. The red graph is the AFM height profile of the few-layer ReS_2 flake. θ is the angle of light polarization (blue arrow) with respect to the crystal b-axis (yellow line). Scale bar, 20 μm. (b−d) The background-subtracted absorption spectra at three different light polarization angles (gray lines). The blue and magenta curves are Lorentzian fits for X_1 and X_2, respectively. (e) θ-dependent spectral weights for X_1 (blue dots) and X_2 (magenta dots). The solid lines are cosine-square function fits.

We first perform light-polarization-dependent absorption measurements on the ReS_2 sample to identify the steady-state optical features of the lowest two excitons, labeled by X_1 and X_2. The light used in the measurements is linearly polarized and its polarization angle (θ) is defined relative to the crystal b-axis of the ReS_2 flake (the yellow line in Figure 2a). Figure 2b−d shows the absorption spectra for X_1 and X_2 at three different angles of θ. We observe that the strength of X_1 is much larger (smaller) than that of X_2 at $\theta = 15°$ ($\theta = 85°$) but comparable at $\theta = 50°$. Their spectral weights are plotted as a function of θ in Figure 3e. There, cosine-square function fittings (solid lines) indicate that the two excitons have different orientations (15° for X_1 and 87° for X_2) which are in good agreement with previous studies.[8,19,27]

Subsequently, we identify the OSE of X_2 by using ultrafast pump−probe spectroscopy. The polarization of the pump (θ_{pu}) is set as X_2's orientation (87°) to maximize the optical Stark shift.[8] The pump photon energy (1.53 eV) is nonresonant with respect to X_2 but close to the resonance energy of X_1, as illustrated in the inset of Figure 3a. This is because we control the incoherent response by superpositioning the polarization-dependent DT spectra for X_1 and X_2, which will be discussed below in detail. Although our experimental condition differs from the usual cases where the pump energy is lower than the energies of the lowest excitons, the OSE is still possible, even when the pump energy is the above exciton energies.[16] Figure 3 displays DT traces

DOI: 10.1021/acs.nanolett.9b03173
Nano Lett. 2019, 19, 7464−7469

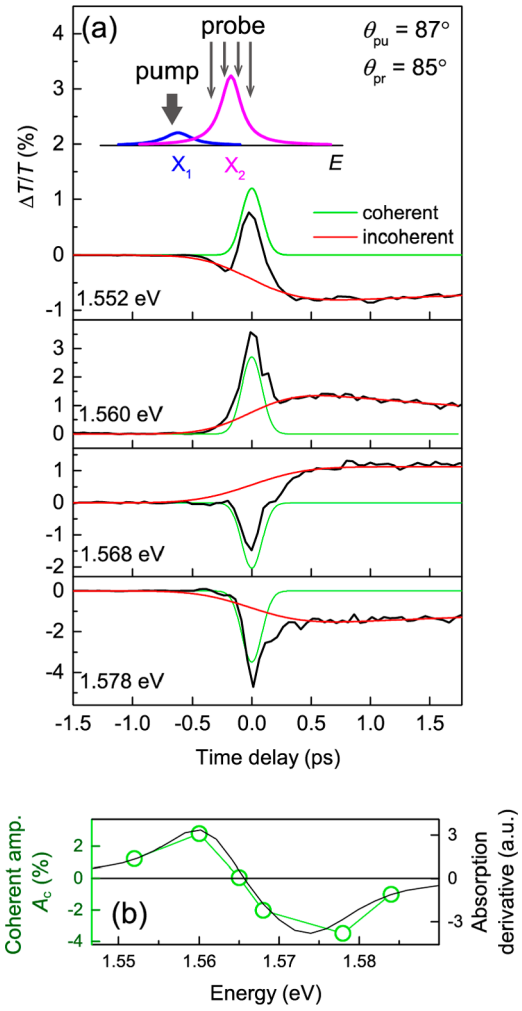

Figure 3. Coherent and incoherent exciton dynamics. (a) DT traces measured at several different probe energies. The polarization of the pump (probe) is θ_{pu} = 87° (θ_{pr} = 85°). Green and red fit lines correspond to the coherent and incoherent components, respectively. Inset: schematic describing pump and probe photon energies (arrows) with absorption profiles for X_1 (blue line) and X_2 (magenta line) at θ_{pr} = 85°. (b) Amplitudes for the coherent component (green dots; left axis) and the first derivative of the absorption near X_2 at θ = 85° (black line; right axis).

measured at several different probe photon energies near X_2. We observe that the Gaussian-like coherent response at Δt = 0 ps (the red lines in Figure 3a) is followed by slow incoherent DT dynamics (the green lines in Figure 3a). To decompose these two components, we fit the DT traces using a simple model that consists of the sum of a Gaussian function for the coherent component and an exponential function for the incoherent component (see Supporting Information Section A). The corresponding fits are shown by green and red lines in Figure 3a. The amplitude of the coherent component exhibits a sign change from negative to positive, whose photon-energy dependence (the green circles in Figure 3b) closely follows the shape of the first derivative of X_2's absorption spectrum (the black line in Figure 3b). This result stems from the blue shift in X_2's absorption resonance (see Figure 1b), confirming the occurrence of the OSE. For the slow incoherent responses, the build-up time constants of ~700 fs are almost independent of the probe photon energy and their decay time constants are in the picosecond time range. The incoherent dynamics can be attributed to exciton broadenings by pump-generated carriers, which will be discussed in the following session. More detailed discussions on carrier/exciton lifetime dynamics in ReS_2 are reported elsewhere[28−31] (Supporting Information Section B).

DT traces in Figure 3a include fairly large incoherent components, as discussed early. The next step was to suppress the incoherent response and control the coherent-to-incoherent ratio by changing the laser polarization. Previously, we already showed that the polarization of the pump determines the amplitude of the coherent part.[8] Thus, we here utilize the polarization of probe to modulate the amplitude of the incoherent component. The polarization of the pump is still set as 87° to maximize the Stark shift in X_2, and the probe energy is fixed at 1.561 eV, an energy at which we can observe large OSE signals (see Figure 3a,b). Figure 4a−e displays the measured DT traces for several different probe polarizations (θ_{pr}). There, we see that the OSE-induced Gaussian-like signals (green fits) are superimposed with slow incoherent responses (red fits). Interestingly, the amplitude of the incoherent response depends largely on θ_{pr} and it is almost completely suppressed at θ_{pr}= 50°, as shown by red lines in Figure 4c (see also inset in Figure 4c). Figure 4f shows the amplitudes of the coherent (A_c, green dots) and incoherent parts (A_{ic}, red dots) as a function of θ_{pr}. A_c is maximized when θ_{pr} is aligned along the orientation of X_2 (~87°). This result is a consequence of the fact that X_2 has the largest transition dipole moment when the light polarization is parallel to its orientation. Importantly, A_{ic} exhibits a sign change at θ_{pr} = 50°, thereby its absolute value is reduced to almost zero. This leads to an extremely large coherent-to-incoherent ratio $|A_c/A_{ic}|$ exceeding ~100, which is 2 orders of magnitude higher than those measured at other polarizations, as shown in Figure 4g. $|A_c/A_{ic}|$ remains greater than 100 at θ_{pr} = 50° when the pump fluence changes (Supporting Information Section C) or a different pump photon energy is used (Supporting Information Section D). This result demonstrates that the incoherent component can be suppressed almost completely by solely using light polarization.

The efficient controllability of $|A_c/A_{ic}|$ originates from the probe polarization dependence of the incoherent response. To understand this, we analyze the DT spectra at several different θ_{pr} for a time delay of Δt = 1.5 ps, a point in the time where only the incoherent component lasts after the rapid coherent dynamics vanishes. The gray lines in Figure 5a−c are DT spectra measured at 15°, 85°, and 50°, angles where A_{ic} exhibits the negative peak, the positive peak, and an intensity of almost zero, respectively. All the spectra exhibit complicated responses, including both positive and negative signs. Such shapes can be explained by the broadenings of exciton resonances.[32] When free carriers and excitons are generated by the pump, they increase the carrier/exciton scattering rate such that the exciton resonance is broadened with respect to its equilibrium line shape, as illustrated in Figure 5d. As a result, the corresponding DT spectrum has a shape similar to the second derivative of the equilibrium resonance (the black line in Figure 5d), which has both positive and negative signs at the center and shoulder of the resonance energy, respectively. At θ_{pr} = 15° (Figure 5a), the negative shoulder of the X_1's absorption-second-derivative-like DT (blue line) has a larger amplitude than the positive component of X_2's response (magenta line), which results in the negative DT signal at the probe energy used in the above trace measurements (1.561 eV; dotted vertical line). This is because X_1 has a much larger

DOI: 10.1021/acs.nanolett.9b03173
Nano Lett. 2019, 19, 7464−7469

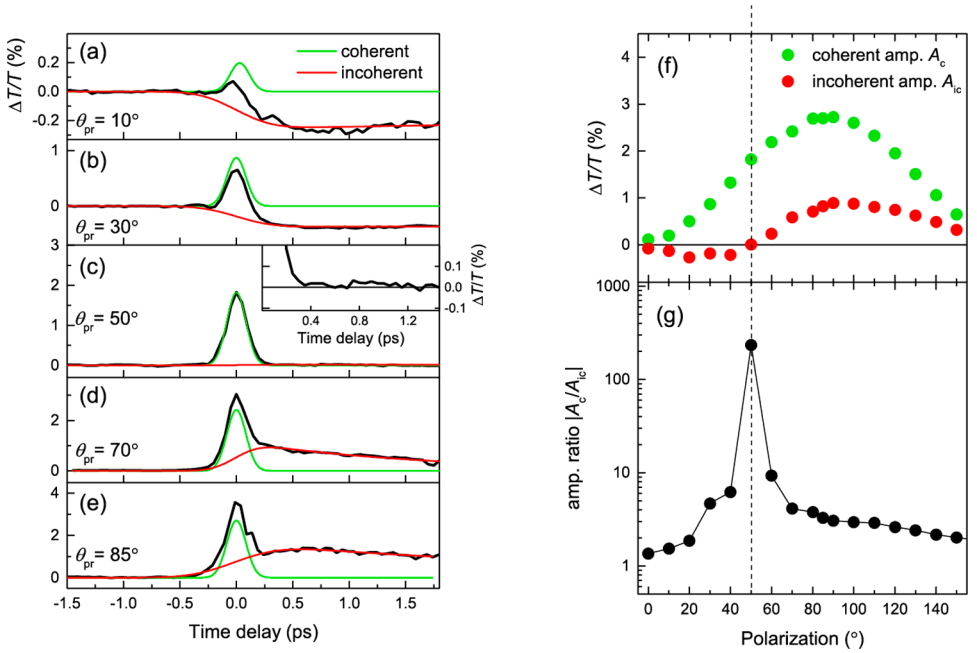

Figure 4. Probe polarization-dependent DT dynamics. (a–e) DT traces measured with varying θ_{pr}. The pump polarization is fixed at θ_{pu} = 87°. Green and red fit lines correspond to the coherent and incoherent components, respectively. Inset of (c) is the zoomed-in view of the incoherent DT dynamics at θ_{pr} = 50°. (f–g) Amplitudes for the coherent and incoherent components are shown by green and red dots, respectively (f), and their θ_{pr}-dependent ratio $|A_c/A_{ic}|$ is shown in (g). The vertical dashed line indicates the probe polarization at which the amplitude ratio has its peak.

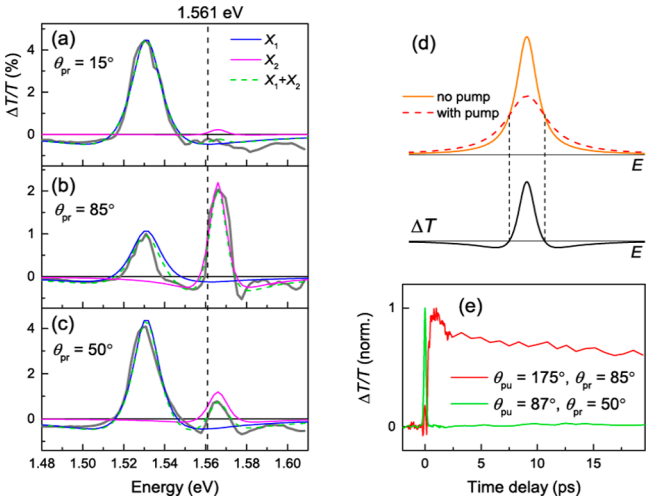

Figure 5. Analysis of incoherent dynamics. (a–c) DT spectra at Δt = 1.5 ps for three different θ_{pr}. The pump polarization is fixed at θ_{pu} = 87°. Blue and magenta lines represent absorption-second-derivative-like DT profiles for X_1 and X_2. Sums of these curves (green dashed lines) accurately fit the measured DT spectra (gray lines). (d) A schematic description for the incoherent differential spectrum. The orange line represents a steady-state absorption resonance for an exciton state, and its broadened line shape by pump excitation is illustrated by the red-dashed line. The black curve shows the corresponding absorption-second-derivative-like DT profile. (e) The DT behaviors at both extremes. The green (red) trace measured at θ_{pu} = 87° and θ_{pr} = 50° (θ_{pu} = 175° and θ_{pr} = 85°) exhibits a strong coherent (incoherent) response and the other is strongly suppressed.

oscillator strength than that of X_2 at θ_{pr} = 15°, as displayed in Figure 2b. Oppositely, at θ_{pr} = 85° where X_2 is stronger than X_1 (Figure 2c), X_2's large positive response leads to a positive DT sign at 1.561 eV, as shown in Figure 5b. Interestingly, at θ_{pr}= 50°, where the oscillator strengths of X_1 and X_2 are comparable to each other (Figure 2d), the negative signal from X_1 cancels out the positive signal from X_2 such that the overall DT is reduced to almost zero at 1.561 eV. These analyses indicate that the suppression of the incoherent component (Figure 4c) was made possible by the superposition of DT responses from the two nondegenerate exciton states with different polarization dependencies. To confirm this interpretation, we performed a similar polarization-dependent experiment on a monolayer ReS_2, where the X_1–X_2 angle difference is smaller than that in the few-layer sample (Supporting Information Section E). The observed maximum $|A_c/A_{ic}|$ in the monolayer (~2) is two-orders of magnitude smaller than that in the few-layer (>100; Figure 4g), further corroborating that the large difference in polarization dependence of the excitons plays a critical role in the observed high $|A_c/A_{ic}|$ in the few-layer ReS_2. The zerolike incoherent response at θ_{pr}= 50° lasts for a much longer duration than 10 ps, as shown by the green line in Figure 5e, implying that the broadening dynamics of X_1 and X_2 have similar time constants. Note that in addition to the exciton broadening the DT spectral shape can be affected by various factors, including peak shifts and changes in spectral weights. However, we do not consider those additional factors, partly for simplicity but primarily because the broadening mainly determines the overall DT lineshapes.[32]

Finally, to determine the limit of the modulation range we intentionally suppress the coherent component and maximize the incoherent response. We set the polarization of the pump as orthogonal to the orientation of X_2 in order to minimize the Stark shift.[8] To maximize the slow incoherent component, we set the probe polarization to 15°, according to the result from Figure 4f. The resultant DT trace is shown by the red line in Figure 5e, whose $|A_c/A_{ic}|$ ratio is ~0.2, which is 3 orders of magnitude lower than the maximum value in Figure 4g. This result demonstrates that it is also possible to intentionally lower the speed of the response by varying laser polarizations.

DOI: 10.1021/acs.nanolett.9b03173
Nano Lett. 2019, 19, 7464–7469

To conclude, we selectively control the femtosecond coherent effect and the picosecond incoherent response of the anisotropic exciton state in a few-layer sample of ReS_2. By using light polarizations, we achieve a coherent-to-incoherent ratio exceeding ~100, which is 3 orders of magnitude higher than the minimum one. This efficient controllability was possible due to the polarization-dependent superposition of differential spectra from two nondegenerate excitons with distinct optical selection rules. The methodology suggested in this work uses only light polarizations to control the coherent/incoherent dynamics of excitons. Although one can try similar modulations by varying the laser wavelength, this approach generally requires complicated nonlinear optical manipulations. Thus, this work provides an efficient method for the realization of ideal ultrafast optoelectronic switches and modulators.

■ ASSOCIATED CONTENT

Supporting Information

The Supporting Information is available free of charge on the ACS Publications website at DOI: 10.1021/acs.nanolett.9b03173.

Fit function for coherent and incoherent DT dynamics, decay dynamics of the incoherent part, pump fluence dependence of DT dynamics, coherent-to-incoherent ratio for a higher pump photon energy, and coherent-to-incoherent ratio in monolayer ReS_2 (PDF)

■ AUTHOR INFORMATION

Corresponding Author

*E-mail: hy.choi@snu.ac.kr.

ORCID

Moon-Ho Jo: 0000-0002-3160-358X

Hyunyong Choi: 0000-0003-3295-1049

Author Contributions

$^{\nabla}$S.S. and D.L. contributed equally.

Notes

The authors declare no competing financial interest.

■ ACKNOWLEDGMENTS

S.S. was supported by the National Research Foundation of Korea (NRF) through the government of Korea (MSIP) (Grant NRF-2019R1F1A1063457). J.L., M.N., H.B., and H.C. were supported by the NRF through the government of Korea (MSIP) (Grant NRF-2018R1A2A1A05079060, the Creative Materials Discovery Program (Grant 2017M3D1A1040828), Scalable Quantum Computer Technology Platform Center (Grant 2019R1A5A1027055), and the Institute for Basic Science (IBS), Korea under Project Code IBS-R014-G1-2018-A1). D.L. and K.L. were supported from the U.S. National Science Foundation (NSF) under Grant CMMI-1825256. M.-H. J. and S. Ch. were supported by the Institute for Basic Science (IBS), Korea (project code IBS-R014-A1).

■ REFERENCES

(1) Liao, P.; Bjorkholm, J. Direct Observation of Atomic Energy Level Shifts in Two-Photon Absorption. *Phys. Rev. Lett.* **1975**, *34*, 1.

(2) Häffner, H.; Gulde, S.; Riebe, M.; Lancaster, G.; Becher, C.; Eschner, J.; Schmidt-Kaler, F.; Blatt, R. Precision Measurement and Compensation of Optical Stark Shifts for an Ion-Trap Quantum Processor. *Phys. Rev. Lett.* **2003**, *90* (14), 143602.

(3) Fröhlich, D.; Nöthe, A.; Reimann, K. Observation of the Resonant Optical Stark Effect in a Semiconductor. *Phys. Rev. Lett.* **1985**, *55*, 1335.

(4) Mysyrowicz, A.; Hulin, D.; Antonetti, A.; Migus, A.; Masselink, W. T.; Morkoç, H. Dressed Excitons" in a Multiple-Quantum-Well Structure: Evidence for an Optial Stark Effect with Femtosecond Response Time. *Phys. Rev. Lett.* **1986**, *56*, 2748.

(5) Von Lehmen, A.; Chemla, D. S.; Zucker, J. E.; Heritage, J. P. Optical Stark Effect on Excitons in GaAs Quantum Wells. *Opt. Lett.* **1986**, *11* (10), 609−611.

(6) Knox, W. H.; Chemla, D. S.; Miller, D. a B.; Stark, J. B.; Schmitt-Rink, S. Femtosecond Ac Stark Effect in Semiconductor Quantum Wells: Extreme Low- and High-Intensity Limits. *Phys. Rev. Lett.* **1989**, *62* (10), 1189−1192.

(7) Sieh, C.; Meier, T.; Jahnke, F.; Knorr, A.; Koch, S. W.; Brick, P.; Hübner, M.; Ell, C.; Prineas, J.; Khitrova, G.; et al. Coulomb Memory Signatures in the Excitonic Optical Stark Effect. *Phys. Rev. Lett.* **1999**, *82* (15), 3112−3115.

(8) Sim, S.; Lee, D.; Noh, M.; Cha, S.; Soh, C. H.; Sung, J. H.; Jo, M. H.; Choi, H. Selectively Tunable Optical Stark Effect of Anisotropic Excitons in Atomically Thin ReS2. *Nat. Commun.* **2016**, *7*, 13569.

(9) Sie, E. J.; McIver, J. W.; Lee, Y.-H.; Fu, L.; Kong, J.; Gedik, N. Valley-Selective Optical Stark Effect in Monolayer WS_2. *Nat. Mater.* **2015**, *14* (3), 290−294.

(10) Kim, J.; Hong, X.; Jin, C.; Shi, S.-F.; Chang, C.-Y. S.; Chiu, M.-H.; Li, L.-J.; Wang, F. Ultrafast Generation of Pseudo-Magnetic Field for Valley Excitons in WSe_2 Monolayers. *Science* **2014**, *346* (6214), 1205−1208.

(11) Yong, C. K.; Horng, J.; Shen, Y.; Cai, H.; Wang, A.; Yang, C. S.; Lin, C. K.; Zhao, S.; Watanabe, K.; Taniguchi, T.; et al. Biexcitonic Optical Stark Effects in Monolayer Molybdenum Diselenide. *Nat. Phys.* **2018**, *14* (11), 1092−1096.

(12) Lamountain, T.; Bergeron, H.; Balla, I.; Stanev, T. K.; Hersam, M. C.; Stern, N. P. Valley-Selective Optical Stark Effect Probed by Kerr Rotation. *Phys. Rev. B: Condens. Matter Mater. Phys.* **2018**, *97* (4), 045307.

(13) Sie, E. J.; Lui, C. H.; Lee, Y.; Fu, L.; Kong, J.; Gedik, N. Large, Valley-Exclusive Bloch-Siegert Shift in Monolayer WS_2. *Science* **2017**, *355*, 1066−1069.

(14) Zhang, W. L.; Li, X. J.; Wang, S. S.; Zheng, C. Y.; Li, X. F.; Rao, Y. J. Polaritonic Manipulation Based on the Spin-Selective Optical Stark Effect in the WS_2 and Tamm Plasmon Hybrid Structure. *Nanoscale* **2019**, *11* (10), 4571−4577.

(15) Giovanni, D.; Chong, W. K.; Dewi, H. A.; Thirumal, K.; Neogi, I.; Ramesh, R.; Mhaisalkar, S.; Mathews, N.; Sum, T. C. Tunable Room-Temperature Spin-Selective Optical Stark Effect in Solution-Processed Layered Halide Perovskites. *Sci. Adv.* **2016**, *2* (6), No. e1600477.

(16) Sie, E. J.; Lui, C. H.; Lee, Y. H.; Kong, J.; Gedik, N. Observation of Intervalley Biexcitonic Optical Stark Effect in Monolayer WS_2. *Nano Lett.* **2016**, *16* (12), 7421−7426.

(17) Tongay, S.; Sahin, H.; Ko, C.; Luce, A.; Fan, W.; Liu, K.; Zhou, J.; Huang, Y. S.; Ho, C. H.; Yan, J.; et al. Monolayer Behaviour in Bulk ReS 2 Due to Electronic and Vibrational Decoupling. *Nat. Commun.* **2014**, *5*, 3252.

(18) Ho, C. H.; Liu, Z. Z. Complete-Series Excitonic Dipole Emissions in Few Layer ReS 2 and ReSe 2 Observed by Polarized Photoluminescence Spectroscopy. *Nano Energy* **2019**, *56*, 641−650.

(19) Aslan, O. B.; Chenet, D. A.; Van Der Zande, A. M.; Hone, J. C.; Heinz, T. F. Linearly Polarized Excitons in Single- and Few-Layer ReS2Crystals. *ACS Photonics* **2016**, *3* (1), 96−101.

(20) Rahman, M.; Davey, K.; Qiao, S. Z. Advent of 2D Rhenium Disulfide (ReS2): Fundamentals to Applications. *Adv. Funct. Mater.* **2017**, *27*, 1606129.

(21) Chenet, D. A.; Aslan, O. B.; Huang, P. Y.; Fan, C.; van der Zande, A. M.; Heinz, T. F.; Hone, J. C. In-Plane Anisotropy in Mono- and Few-Layer ReS2 Probed by Raman Spectroscopy and Scanning Transmission Electron Microscopy. *Nano Lett.* **2015**, *15* (9), 5667−5672.

DOI: 10.1021/acs.nanolett.9b03173
Nano Lett. 2019, 19, 7464−7469

(22) Arora, A.; Noky, J.; Drüppel, M.; Jariwala, B.; Deilmann, T.; Schneider, R.; Schmidt, R.; Del Pozo-Zamudio, O.; Stiehm, T.; Bhattacharya, A.; et al. Highly Anisotropic In-Plane Excitons in Atomically Thin and Bulklike 1T′-$ReSe_2$. *Nano Lett.* **2017**, *17*, 3202−3207.
(23) Kim, B. S.; Kyung, W. S.; Denlinger, J. D.; Kim, C.; Park, S. R. Strong One-Dimensional Characteristics of Hole-Carriers in ReS_2 and $ReSe_2$. *Sci. Rep.* **2019**, *9*, 2730.
(24) Ho, C. H.; Wut, C. S.; Huang, Y. S.; Liao, P. C.; Tiong, K. K. Temperature Dependence of Energies and Broadening Parameters of the Band-Edge Excitons of ReS_2 and $ReSe_2$. *Phys. Rev. B: Condens. Matter Mater. Phys.* **1997**, *55*, 15608.
(25) An, C.; Xu, Z.; Shen, W.; Zhang, R.; Sun, Z.; Tang, S.; Xiao, Y. F.; Zhang, D.; Sun, D.; Hu, X.; et al. The Opposite Anisotropic Piezoresistive Effect of ReS_2. *ACS Nano* **2019**, *13* (3), 3310−3319.
(26) Xiong, Y.; Chen, H. W.; Zhang, D. W.; Zhou, P. Electronic and Optoelectronic Applications Based on ReS_2. *Phys. Status Solidi RRL* **2019**, *13*, 1800658.
(27) Sim, S.; Lee, D.; Trifonov, A. V.; Kim, T.; Cha, S.; Sung, J. H.; Cho, S.; Shim, W.; Jo, M.-H.; Choi, H. Ultrafast Quantum Beats of Anisotropic Excitons in Atomically Thin ReS_2. *Nat. Commun.* **2018**, *9*, 351.
(28) Cui, Q.; He, J.; Bellus, M. Z.; Mirzokarimov, M.; Hofmann, T.; Chiu, H. Y.; Antonik, M.; He, D.; Wang, Y.; Zhao, H. Transient Absorption Measurements on Anisotropic Monolayer ReS_2. *Small* **2015**, *11* (41), 5565−5571.
(29) Wang, X.; Shinokita, K.; Lim, H. E.; Mohamed, N. B.; Miyauchi, Y.; Cuong, N. T.; Okada, S.; Matsuda, K. Direct and Indirect Exciton Dynamics in Few-Layered ReS_2 Revealed by Photoluminescence and Pump-Probe Spectroscopy. *Adv. Funct. Mater.* **2019**, *29* (6), 1806169.
(30) Dhakal, K. P.; Kim, H.; Lee, S.; Kim, Y.; Lee, J. D.; Ahn, J. H. Probing the Upper Band Gap of Atomic Rhenium Disulfide Layers. *Light: Sci. Appl.* **2018**, *7* (1), 98.
(31) Liu, F.; Zhao, X.; Yan, X. Q.; Xie, J.; Hui, W.; Xin, X.; Liu, Z. B.; Tian, J. G. Ultrafast Nonlinear Absorption and Carrier Relaxation in ReS_2 and $ReSe_2$ Films. *J. Appl. Phys.* **2019**, *125*, 173105.
(32) Sim, S.; Park, J.; Song, J. G.; In, C.; Lee, Y. S.; Kim, H.; Choi, H. Exciton Dynamics in Atomically Thin MoS_2: Interexcitonic Interaction and Broadening Kinetics. *Phys. Rev. B: Condens. Matter Mater. Phys.* **2013**, *88*, 075434.

DOI: 10.1021/acs.nanolett.9b03173
Nano Lett. 2019, 19, 7464−7469